AGU PUBLICATIONS

JGR

Journal of Geophysical Research: Atmospheres

RESEARCH ARTICLE
10.1002/2015JD024001

Key Points:
- T-TREC-retrieved wind and radial velocity data are assimilated using an ensemble Kalman filter
- The relative impacts of two data sets on analysis and prediction changes with assimilation windows
- The combination of retrieved wind and radial velocity produces better analyses and forecasts

Correspondence to:
M. Xue,
mxue@ou.edu

Citation:
Wang, M., M. Xue, and K. Zhao (2016), The impact of T-TREC-retrieved wind and radial velocity data assimilation using EnKF and effects of assimilation window on the analysis and prediction of Typhoon Jangmi (2008), *J. Geophys. Res. Atmos.*, *121*, 259–277, doi:10.1002/2015JD024001.

Received 27 JUL 2015
Accepted 16 DEC 2015
Accepted article online 20 DEC 2015
Published online 15 JAN 2016

The impact of T-TREC-retrieved wind and radial velocity data assimilation using EnKF and effects of assimilation window on the analysis and prediction of Typhoon Jangmi (2008)

Mingjun Wang[1,2], Ming Xue[1,2,3], and Kun Zhao[1]

[1]Key Laboratory for Mesoscale Severe Weather/MOE and School of Atmospheric Science, Nanjing University, Nanjing, China, [2]Center for Analysis and Prediction of Storms, Norman, Oklahoma, USA, [3]School of Meteorology, University of Oklahoma, Norman, Oklahoma, USA

Abstract This study examines the relative impact of assimilating T-TREC-retrieved winds (V_{TREC}) versus radial velocity (V_r) on the analysis and forecast of Typhoon Jangmi (2008) using an ensemble Kalman filter (EnKF). The V_{TREC} and V_r data at 30 min intervals are assimilated into the ARPS model at 3 km grid spacing over four different assimilation windows that cover, respectively, 0000–0200, 0200–0400, 0400–0600, and 0000–0600 UTC, 28 September 2008. The assimilation of V_{TREC} data produces better analyses of the typhoon structure and intensity than the assimilation of V_r data during the earlier assimilation windows, but during the later assimilation windows when the coverage of V_r data on the typhoon from four Doppler radars is much improved, the assimilation of V_r outperforms V_{TREC} data. The combination of V_{TREC} and V_r data, either by assimilating both V_{TREC} and V_r data in all cycles or by assimilating V_{TREC} in the first cycle and V_r in the remaining cycles (labeled V_{TFVR}), further improves the analyses of the typhoon structure and intensity compared to assimilating V_{TREC} or V_r data alone. Quantitative verifications of 24 h forecasts of the typhoon show that the V_{TFVR} assimilation experiments produces forecasts that best match the best track data and also have the highest precipitation prediction skills. The track forecast errors in experiment that assimilate V_{TREC} data through the later cycles are the largest. The behaviors are discussed based on the coverage, information content, and accuracy of the various forms of data.

1. Introduction

Ground-based Doppler radars provide three-dimensional wind and precipitation observations of tropical cyclones (TCs) at high temporal and spatial resolution when TCs move within the range of coastal radars. These observations help improve our understanding of important processes within the TC inner core and the outer rainbands [*Blackwell*, 2000; *Corbosiero et al*., 2006; *Hong and Chang*, 2005; *Lee et al*., 2000; *Lee and Bell*, 2007; *Zhao et al*., 2008]. Efforts have been made to assimilate the radial velocity (V_r) and reflectivity (Z) from ground-based Doppler radars into high-resolution numerical weather prediction model to improve the TC forecasts and the data assimilation (DA) methods used include the three-dimensional variational (3DVAR) method [*Xiao et al*., 2007; *Zhao and Xue*, 2009; *Zhao et al*., 2012; *Zhao and Jin*, 2008], the ensemble Kalman filter (EnKF) [*Dong and Xue*, 2013; *Xue and Dong*, 2013; *Zhang et al*., 2009], and the ensemble variational hybrid method [*Li et al*., 2012]. Results have shown that the assimilation of V_r and/or Z has positive impacts on TC intensity and track forecasting.

For typical S band operational weather surveillance radars, e.g., the Weather Surveillance Radar-1988 Doppler of the United States and the China New Generation Radar-1998 Doppler of China, the maximum range of Z observations is about twice as that of V_r. By tracking the motion of radar echo, the T-TREC technique [*Wang et al*., 2011] can produce retrieved winds (V_{TREC}) with a much larger coverage than V_r data. The inner core TC circulation can be captured much sooner by the retrieved V_{TREC} than V_r when a TC approaches a coastal radar [*Wang et al*., 2011]. This reflectivity-derived V_{TREC} also has both radial and cross-beam wind components and therefore contains more complete wind information than V_r. The assimilation of V_{TREC} into numerical models thus has the potential to improve the TC forecasts at a longer lead time and to enable earlier warnings to the coastal community. The drawback with the T-TREC data is that they have lower spatial resolutions (10 km) than *Vr* data (~250 m).

Two recent studies examined the impact of V_{TREC} assimilation on the analyses and forecasts of typhoons [*Li et al*., 2013; *Wang et al*., 2014, W14 hereafter]. *Li et al*. [2013] assimilated V_{TREC} data using the Weather Research and Forecast 3DVAR system [*Barker et al*., 2004; *Xiao et al*., 2005] for Typhoon Meranti (2010) before it made landfall in Fujian Province of China. V_{TREC} or V_r data from a coastal radar were assimilated for single time assimilations at different lead times. Results show that V_{TREC} DA generally produced better analyses of the typhoon structure and intensity than direct assimilation of V_r data. The subsequent forecasts for the typhoon track, intensity, structure, and precipitation were also better, although the differences became smaller for the latter analysis times when V_r data coverage improved as the typhoon approached the radar.

W14 examined the impacts of V_{TREC} data through cycled DA using EnKF for Typhoon Jangmi (2008) that passed over the northern part of the Taiwan Island. Cycled assimilation of V_{TREC} data retrieved from the radar located at Hualian, Taiwan, produced more significant improvements to the analysis and forecast of Jangmi's intensity and structure than V_r data with the same 3 hour assimilation window. Sensitivity experiments show that V_{TREC} DA built up a reasonably strong vortex in 1 h, while longer assimilation windows were required for V_r assimilation to realize similar effects. Though the difference assimilating the two data types decreased when the assimilation window became longer, the superior performance of V_{TREC} assimilation was still evident.

In W14, the Hualian radar V_r or V_{TREC} were assimilated from 0000 to 0300 UTC 28 September 2008 when the center of Jangmi was still far from the Taiwan Island and only part of its inner core region was captured by the radar. With Jangmi moving closer to the Taiwan Island, more of its inner core is within the coverage of the V_r data of the Hualian and additional Taiwan operational radars. With such changes, the relative impacts of assimilating V_r or V_{TREC} may also change, but the dependency of the impact on assimilation window has not been investigated in published studies, as far as we know.

When a TC or its inner core move into the range of Z (~460 km), assimilating V_{TREC} data can help build up the vortex early. After the TC gets closer to land and falls into the range of V_r data (~230 km), it is possible to assimilate both V_r and V_{TREC} together. Advantages over assimilating V_r or V_{TREC} individually are expected because V_r data have finer spatial resolutions and contain more detailed structures, while V_{TREC} data also contain retrieved cross-beam component and have larger spatial coverage (W14). Being mainly derived from Z data, V_{TREC} is independent of V_r. The impact of assimilating both V_r and V_{TREC} has not been examined in previously published studies.

Therefore, as a natural extension of W14, we examine in this study the relative impact of assimilating V_r, or V_{TREC} or both in DA windows with different lengths and lead times (relative to landfall), on the analysis and forecasting of Typhoon Jangmi, using data from up to four radars over the Taiwan Island. The EnKF DA method will again be used. In addition, a "hybrid" configuration is also tested in which V_{TREC} data are assimilated in the first cycle, while V_r data are assimilated in the later cycles. This study aims to provide guidance on the optimal utilization of the two types of radar data for improving TC track and intensity forecasting near TC landfall.

The rest of this paper is organized as follows. Section 2 describes the forecast model, radar data, and experimental design. The individual impacts of V_{TREC} and V_r from single or multiple radars in different assimilation windows are discussed in section 3. Section 4 presents the results assimilating V_{TREC} and V_r together using various configurations. Quantitative verifications for track, intensity, and precipitation from all experiments are given in section 5. Conclusions and discussions are given in section 6.

2. Model, Radar Data, and Experimental Design

2.1. The Prediction Model

The prediction model and its configuration follow W14. The Advanced Regional Prediction System [ARPS; *Xue et al*., 2000, 2001] is used as the prediction model. The physical domain is $2400 \times 2400 \times 25$ km^3 and has a 3 km horizontal grid spacing (Figure 1). The mean vertical grid spacing is 500 m with the grid spacing near the surface being 20 m. Model physics include the Lin ice microphysics scheme [*Lin et al*., 1983], Goddard Space Flight Center long- and short-wave radiation parameterization, a two-layer force-restore soil-vegetation model [*Ren and Xue*, 2004], 1.5-order turbulent kinetic energy-based subgrid-scale turbulence [*Deardorff*, 1980], and planetary boundary layer parameterization [*Xue et al*., 1996].

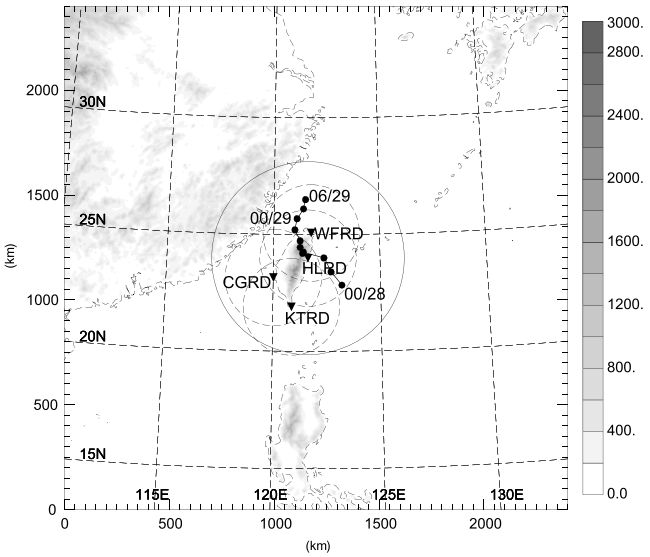

Figure 1. The physical domain of the numerical simulation, with the average best track (see section 2) locations plotted every 3 h from 0000 UTC 28 to 0600 UTC 29 September 2008 (marked by black dots). The triangles denote the positions of radar stations, and their radial velocity observation range is shown by the dashed circles. The solid circle indicates the maximum reflectivity range of HLRD. The gray shading shows the terrain height (m). This figure is adapted from *Wang et al*. [2014].

2.2. Radar Data Processing and Quality Control

Four operational S band radars of Taiwan (Figure 1), including those at Hualian (HLRD), Wufenshan (WFRD), Kenting (KTRD), and Chigu (CGRD), are used in this study. V_r and Z data are first manually edited to dealiase radial velocity and remove ground clutter. For V_r assimilation, the V_r data are interpolated in the horizontal to the ARPS model columns but kept on the elevation levels in the vertical. The processing and use of the V_{TREC} data generally follows W14. V_{TREC} is retrieved from reflectivity data from HLRD between 0000 and 0600 UTC 28 September 2008 every 30 min. HLRD in this case was closest to the typhoon and provided the best data coverage. T-TREC analyses are performed within a 300 km radius of the typhoon center from 1 to 8 km with a vertical spacing of 1 km. The horizontal grid spacing of V_{TREC} is 10 km, and the retrieved wind data are directly assimilated. More details on the T-TREC technique can be found in *Wang et al*. [2011].

To assess the reliability of the retrieved V_{TREC} data, the percentage cumulative histogram of the absolute differences between observed V_r and the radial component of the V_{TREC} at all V_r data levels from 0000 UTC to 0600 UTC 28 September 2008 are shown in Figure 2a. The scatterplot of the data pairs is shown as an inset

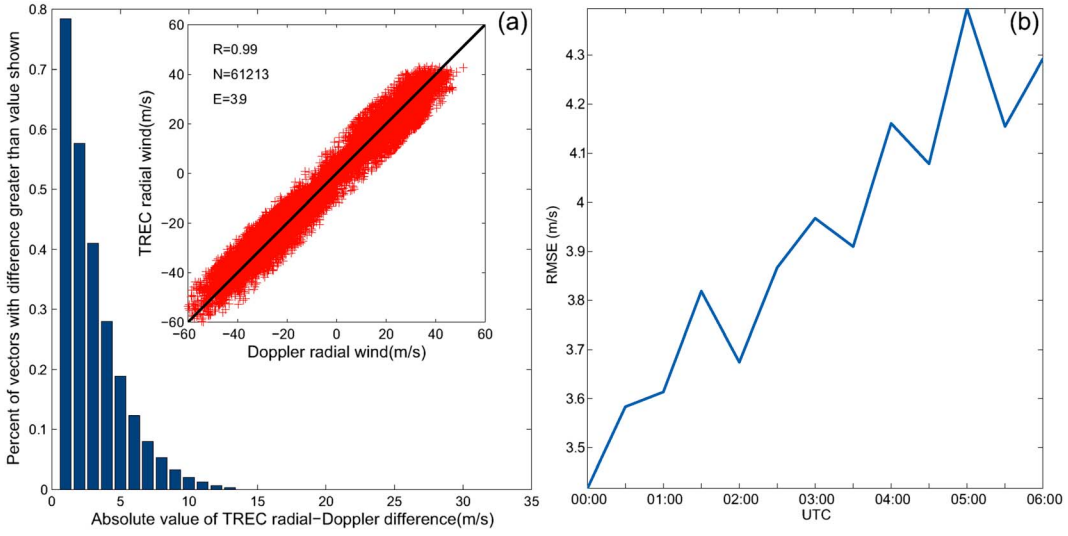

Figure 2. (a) Percentage cumulative histogram of the difference between observed Doppler radar radial velocities and the radial component of T-TREC-retrieved winds for Typhoon Jangmi from 0000 UTC to 0600 UTC 28 September 2008, every 30 min. Insert in upper right shows a scatterplot of retrieved radial velocity versus radial velocity measurements. *N* is the total number of radial velocity samples. *R* and *E* represent the correlation coefficient and the root-mean-square difference (RMSD), respectively. (b) RMSD between measured Doppler radial velocities and the radial component of T-TREC-retrieved winds from 0000 UTC to 0600 UTC every 30 min.

Table 1. Summary of Experiments With and Without Radar Data Assimilation Using Different Observations Types, the Number of Radars, and Assimilation Periods

Groups	Experiments	Observations Assimilated	Assimilation Period
CNTL	CNTL	No DA	NA
VrHL	VrHL06	V_r from HLRD	0000–0600 UTC
	VrHL02		0000–0200 UTC
	VrHL24		0200–0400 UTC
	VrHL46		0400–0600 UTC
Vr4RD	Vr4RD06	V_r from four radars	0000–0600 UTC
	Vr4RD02		0000–0200 UTC
	Vr4RD24		0200–0400 UTC
	Vr4RD46		0400–0600 UTC
TREC	TREC06	V_{TREC}	0000–0600 UTC
	TREC02		0000–0200 UTC
	TREC24		0200–0400 UTC
	TREC46		0400–0600 UTC
TRECVr	TRECVr06	$V_{TREC} + V_r$ from four radars	0000–0600 UTC
	TRECVr02		0000–0200 UTC
	TRECVr24		0200–0400 UTC
	TRECVr46		0400–0600 UTC
TFVR	TFVR06	V_{TREC} for the first cycle and V_r for the rest of cycles	0000–0600 UTC
	TFVR02		0000–0200 UTC
	TFVR24		0200–0400 UTC
	TFVR46		0400–0600 UTC

of the figure. The percentage of differences less than 4 m s^{-1} is over 70%, while the average root-mean-square difference (RMSD) is 3.9 m s^{-1}. The scatterplot shows a uniform distribution along the diagonal with the correlation coefficient between observed V_r and the radial component of V_{TREC} being 0.99 (Figure 2a), indicating no bias with the independent V_{TREC} retrieval. The RMSDs at different times of the 6 h period are also plotted in Figure 2b. There is a general increase of RMSD from about 3.4 m s^{-1} at 0000 UTC to about 4.3 m s^{-1} at 0600 UTC as Jangmi approached Taiwan Island. The closer is Jangmi to the island, the less valid is the conserved reflectivity advection assumption of the T-TREC method due to the new convection triggering induced by the interaction between the TC and terrain including the Central Mountain Range of Taiwan (Figure 1), which leads to larger retrieval errors. Overall, the time-averaged RMSD of about 3.9 m s^{-1} is acceptable, which is consistent with the corresponding error statistics of less than 4 m s^{-1} from data samples examined in *Wang et al*. [2011]. Based on the above discussion on observation error statistics, standard deviations for V_r and V_{TREC} are specified as 2 m s^{-1} and 5 m s^{-1}, respectively, the same as W14, in the EnKF DA.

2.3. EnKF Experimental Design

Five groups of experiments are conducted to examine the individual and combined impact of V_r and V_{TREC} (Table 1). "VrHL," "Vr4RD," and "TREC" assimilate V_r from HLRD only (V_{HL}), V_r from all four radars (V_{4RD}), and V_{TREC}, respectively (Table 1). "TRECVr" assimilates both V_{4RD} and V_{TREC} data at each cycle. In "TFVR," V_{TREC} data are assimilated in the first cycle, and V_{4RD} data are assimilated in the remaining cycles. Studies [*Li et al*., 2013; W14] have demonstrated that even single time assimilation of V_{TREC} can be effective in building up the TC vortex. The continuous cycles of V_{4RD} data can potentially provide more detailed structures.

The 6 h period from 0000 to 0600 UTC is divided into three stages according to the V_r coverage for Jangmi (Figure 1). In the first two hours (0000 to 0200 UTC), the inner core region of Jangmi is only partly covered by the V_r data of HLRD. From 0200 to 0400 UTC, the inner core is fully observed by HLRD and partly observed by WFRD (Figure 1). In the last two hours (0400 to 0600 UTC), the inner core is fully covered by HLRD and WFRD. All the aforementioned five groups of experiments (including VrHL, Vr4RD, TREC, TRECVr, and TFVR) are performed with four different assimilation windows (AWs), which cover, respectively, 0000 to 0600 UTC (AW06), 0000 to 0200 UTC (AW02), 0200 to 0400 UTC (AW24), and 0400 to 0600 UTC (AW46). The digital suffices in the experiment names, i.e., "06," "02," "24," and "46," indicate the four different AWs (Table 1). At the end of the DA window of each experiment, a deterministic forecast is launched and run through 0600 UTC 29 September 2008. The experiments with the DA window suffix "02" share the same DA configuration with the experiments with suffix "06" during the first two hours, but their forecasts start earlier at 0200 UTC. Apart from the DA

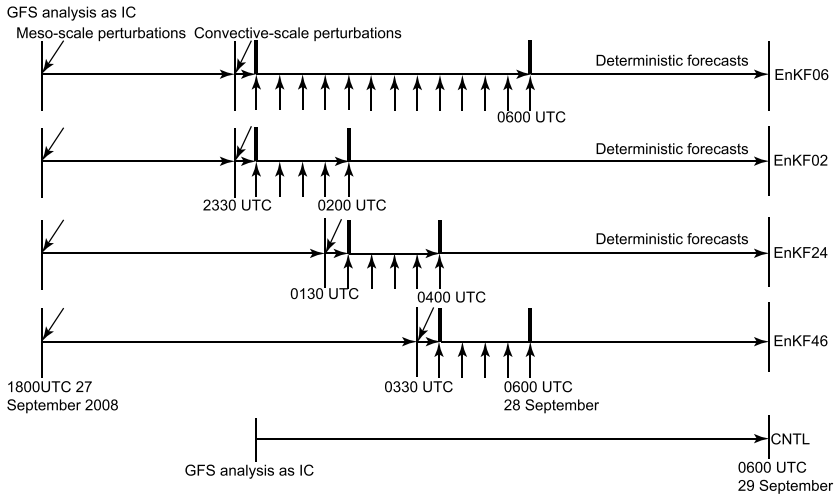

Figure 3. The EnKF data assimilation and forecast schemes, along with CNTL. The vertical arrows denote the assimilation of radar data, and the slanted arrows denote the perturbations added to generate the ensemble members.

experiments, a baseline control forecast (CNTL) without radar DA runs from 0000 UTC 28 September to 0600 UTC 29 September 2008, initialized from the operational National Centers for Environmental Prediction GFS analysis.

Similar to W14, an initial 40-member ensemble is created by adding mesoscale perturbations to the GFS analysis at 1800 UTC 27 September. Convective-scale perturbations are further introduced into the ensemble forecasts 30 min before the first radar DA, e.g., at 2330 UTC 27 September for AW06 and AW02, 0130 UTC 28 September for AW24, and 0330 UTC 28 September for AW46 (see Figure 3). The configurations of perturbations are the same as W14. The DA schemes are illustrated in Figure 3.

The same as W14, covariance localization radii of 50 (10) km in the horizontal and 4 km in the vertical are chosen when assimilating V_{TREC} (V_r) data. A posterior relaxation-to-prior adaptive covariance inflation [*Whitaker and Hamill*, 2012] with $\alpha = 0.9$ is applied at those model grid points directly influenced by observations to help maintain the ensemble spread. Localization and inflation parameters are chosen based on the experience obtained from *Dong and Xue* [2013] and a set of sensitivity experiments.

3. Individual Assimilation of V_{TREC} or V_r With Different Assimilation Windows

In this section, the relative impacts of assimilating V_{TREC}, V_{HL}, or V_{4RD} data on the intensity and structure analyses for different AWs are examined. The analyses considered in the following are the ensemble means.

The minimum sea level pressures (MSLPs) and maximum surface winds (MSWs) during the assimilation cycles for four AWs from VrHL, Vr4RD, and TREC groups are plotted in Figure 4, along with the average best track (ABT) data from the Japan Meteorological Agency, Taiwan Central Weather Bureau, and Joint Typhoon Warning Center. The ±1 standard deviation of the mean best track data are also plotted, encompassing the gray areas. The use of the average is to reduce uncertainty with the best track data, as was done in W14.

The V_{HL} data coverage for Jangmi is improved as the distance of Jangmi from land is decreased in the later assimilation windows. As a result, the assimilation of V_{HL} improves the analysis more effectively with closer distances: the maximum MSLP reduction increases from 9.6 hPa in VrHL02 to 26.3 hPa in VrHL24 (Figure 4a). Compared to V_{HL} data, V_{4RD} data provide better coverage on Jangmi's inner core, especially in the later time period from 0400 to 0600 UTC (see Figure 1). The final analyzed MSLP differences between VrHL and Vr4RD are 5.5 hPa, 8.2 hPa, and 12.5 hPa for AW02, AW24, and AW46, respectively. When Jangmi's inner core falls into the range of V_{4RD} completely in window "46," the MSLP reduction of V_{4RD} assimilation at 0500 UTC is clearly larger than the small changes in the earlier windows and the final analyzed MSLP is around 940 hPa, close to the best track value of 930 hPa.

For all three 2 h AWs, the experiments assimilating V_{TREC} always have the strongest analyzed vortices compared to assimilating V_r from either one or four radars. The MSLP evolutions from V_{TREC} assimilation experiments in

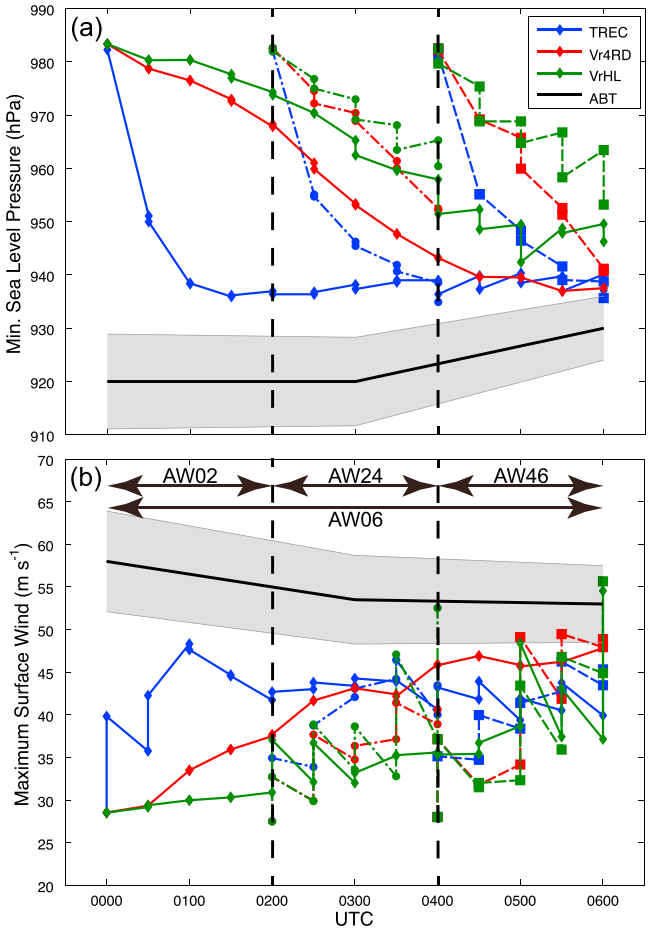

Figure 4. Analysis and forecast (a) minimum sea level pressures and (b) maximum surface winds during the analysis cycles from experiment groups VrHL (blue lines), Vr4RD (red lines), and TREC (green lines) for assimilation windows of 0000 to 0600 UTC (solid lines), 0200 to 0400 UTC (dash-dotted lines), and 0400 to 0600 UTC (dashed lines). Assimilation windows (AWs) are marked by the two-way arrows. The average best track data are plotted in bold black for comparison. The gray shading indicates the ±1 standard deviation centered at the averaged best track.

three different assimilation windows are similar with each other. The final MSLPs are always around 935 to 937 hPa (Figure 4a). Consequently, the final analysis differences between assimilating V_{HL} and V_{TREC} decrease from 35 hPa and 25 hPa to 14 hPa in three assimilation windows as Jangmi moved closer to land (Figure 4a). When V_{HL}, V_{4RD}, or V_{TREC} data are assimilated continuously from 0000 through 0600 UTC, the advantage of assimilating V_{TREC} over V_r data is much decreased. The final MSLP differences between assimilating V_{TREC} and V_{HL} or V_{4RD} are about 8 hPa and 0.5 hPa respectively, with the 6 h AW.

Consistent with MSLP analyses, the analyzed MSWs of VrHL or Vr4RD experiments generally increase as Jangmi moved closer to Taiwan in later assimilation windows (Figure 4b), due to the improved V_r coverage on the TC, both in the horizontal and at lower levels (<1 km). The final analyzed MSWs of VrHL experiments are closer or even stronger than the ABT MSW of 54 m s^{-1} in AW24, AW4, and AW06. The analyzed MSWs of Vr4RD24, Vr4RD46, and Vr4RD06 in later cycles are at least 7 m s^{-1} lower than those in VrHL24, VrHL46, and VrHL06. When the analysis has to be fit to more observations, the fit to individual observations tends to be poorer; this appears to be a reason for the lower values of the analyzed MSW. This can be seen more clearly between the MSWs of VrHL and Vr4RD during 0000–0200 UTC (Figure 4b).

The analyzed MSWs of TREC experiments for all three 2 h windows are close to each other with their final MSWs being between 43 and 45 m s^{-1} (Figure 4b), approximately 10 m s^{-1} below the ABT values. At 0600 UTC, they are generally within 2 standard deviations of the ABT values. As pointed out in W14, this difference can be attributed to the underestimation of maximum wind speed in V_{TREC} data due to the relative smoothness of their fields [*Tuttle and Gall*, 1999; *Wang et al.*, 2011].

Overall, the intensity analyses from V_{TREC} assimilation are not sensitive to the AWs used since the inner core is quite well covered by V_{TREC} throughout the 6 h period. The assimilation of V_{TREC} is able to establish a strong vortex in a short period (<1 h) as evidenced by the sharp reduction of MSLP in the first two 30 min cycles, which is mostly achieved via model adjustment during the forecast period (Figure 4a). The fact that the retrieved V_{TREC} better represents the closed vortex circulation significantly accelerates the model adjustment of pressure toward the analyzed wind circulation. This point as well as the pressure-wind adjustment process was discussed in detailed in *Wang et al.* [2014].

The analyzed intensity from V_r data is clearly better toward the end of the 6 h period, as more V_r data become available. When only V_r data from the single Hualian radar are assimilated, it takes the full 6 h AW for the

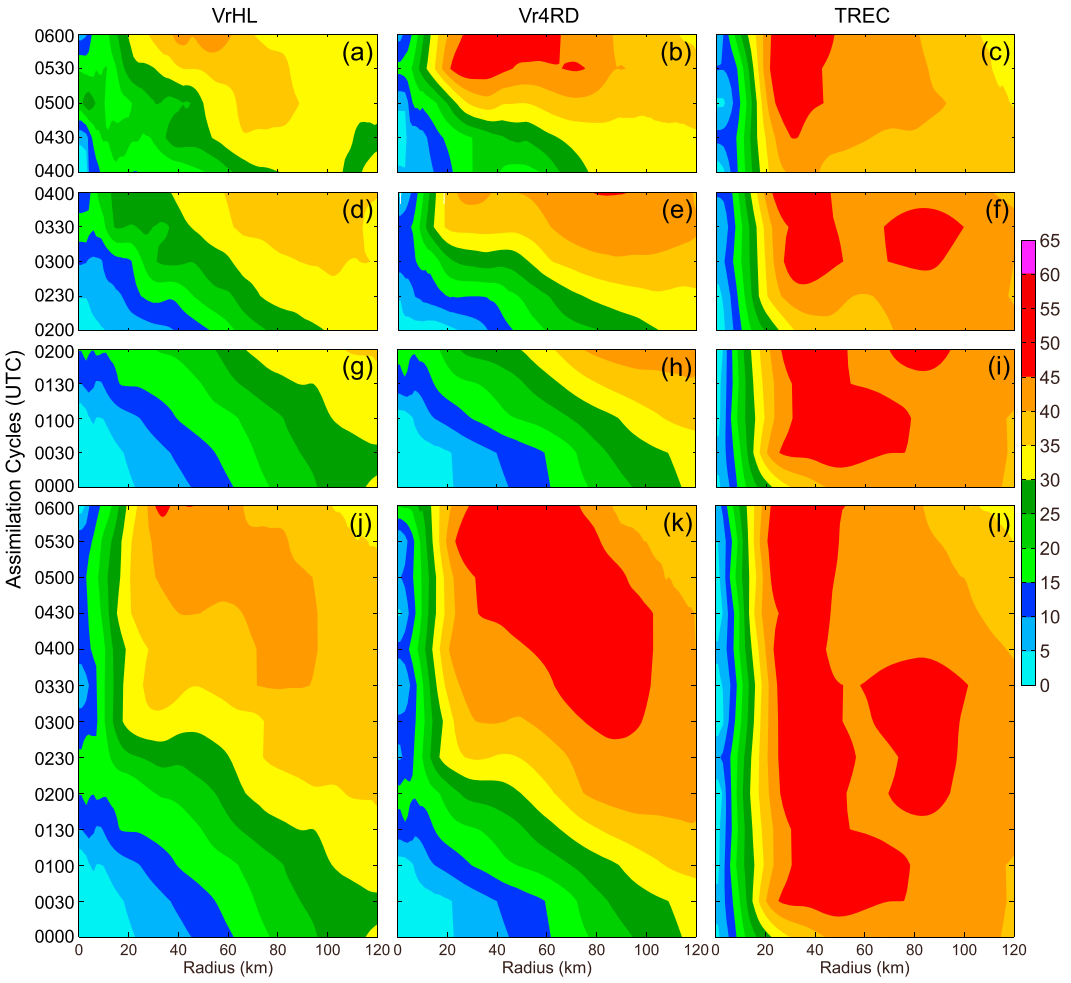

Figure 5. Time-radius Hovmöller diagrams of azimuthally averaged tangential wind speed (m s^{-1}) at 500 m height for the analyses in different assimilation windows, for the three groups of experiments: (a, d, g, and j) the VrHL-assimilating group, (b, e, h, and k) theVr4RD group, and (c, f, i, and l) the TREC group.

analyzed TC to reach an adequate intensity. When V_r data from all four radars are assimilated, a 2 h AW at the end is sufficient. The analyzed intensities in Vr4RD46 and Vr4RD06 are actually stronger than the corresponding V_{TREC} experiments and are closer to the ABT data. Given the ability for V_{TREC} data to quickly establish an intense typhoon vortex, and the ability of V_r data in giving more accurate typhoon intensity after sufficient data are assimilated, it appears beneficial if both types of data are assimilated together. After all, they are independent forms of observations. This will be examined in section 4.

To see more clearly how the intensity of the analyzed typhoon vortex changes within the assimilation windows, we show in Figure 5 time-radius Hovmöller diagrams of the analyzed azimuthally averaged tangential wind speed at 500 m height during the assimilation cycles from three groups of experiments: those that assimilate V_{HL}, V_{4RD}, and V_{TREC} data, respectively. The analyzed vortices from V_{HL} assimilation intensify slowly during assimilation cycles in all four different windows (Figures 5a, 5d, 5g, and 5j). The low-level circulations are weak and broad with the maximum wind speed barely exceeding 40 m s^{-1} and a large radius of maximum wind (RMW) of about 80 km before 0400 UTC. After 0400 UTC, the low-level vortex intensifies quickly with the strongest wind exceeding 45 m s^{-1} and the radius of RMW decreased to about 40 km and benefits from the better V_r data coverage. The analyzed vortex in Vr4RD experiments strengthens faster than in VrHL experiments in terms of the wind speed and RMW, especially during the later AWs in Vr4RD46 and Vr4RD06, when Jangmi's inner core is covered by multiple radars (Figures 5b, 5e, 5h, and 5k). We note here that the analyzed MSW is sensitive to local perturbations in the wind fields; their values are not the best indicator of the vortex intensity. In

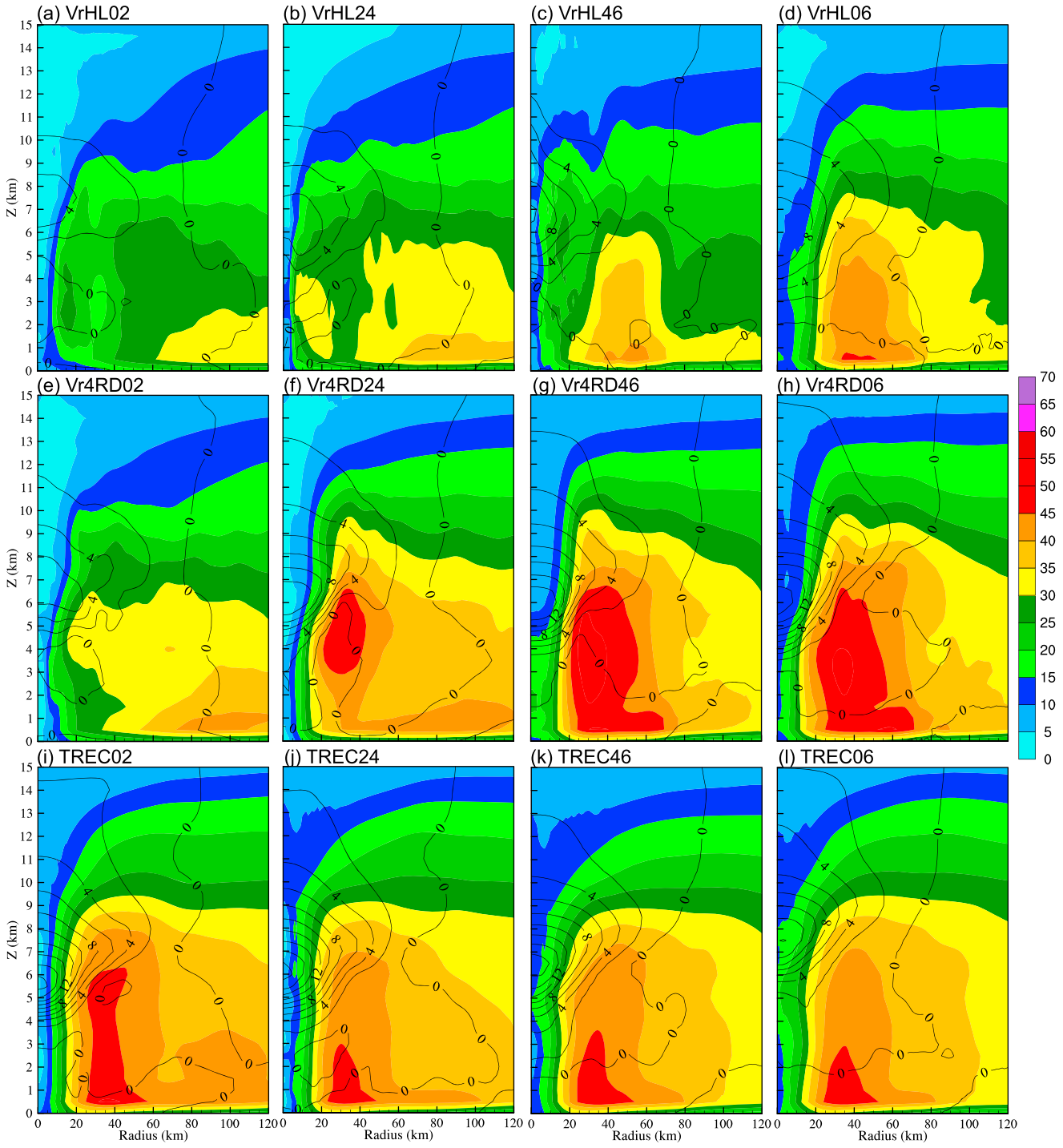

Figure 6. Azimuthally averaged tangential wind speed (color shaded) and temperature anomaly (contours with intervals of 2 K), from the final analyses of (a–d) VrHL group, (e–h) Vr4RD group, and (i–l) TREC group.

comparison, the azimuthally averaged tangential wind speed represents the intensity of vortex circulation better and generally has relation with the MSLP when a balance between the wind and pressure fields are reached (usually through model adjustments during the assimilation cycles as discussed in *Wang et al.* [2014]). The final analyzed tangential winds of Vr4RD experiments are much stronger than those of VrHL experiments, which is consistent with the lower MSLP values. In general, V_{TREC} assimilation helps to build a reasonably strong vortex with strong winds over 45 m s^{-1} and a RMW of about 35 km in 1 h (Figures 5c, 5f, 5i, and 5l).

To see the vertical structure of analyzed vortices, the final analyzed azimuthally averaged tangential wind speed and horizontal temperature anomaly from the VrHL, Vr4RD, and TREC groups are presented in Figure 6. The temperature anomaly is defined as the deviation from the horizontal average within a 180 km radius [*Liu et al.*, 1999]. The VrHL experiments all have a weak, broad, and relatively shallow vortex. The warm core anomalies are less than 8 K, and the 40 m s^{-1} contours are all below 6 km (Figures 6a–6d). The axisymmetric circulations are stronger and warm core anomalies are more intense in Vr4RD experiments than the corresponding VrHL experiments. In the experiments with AW02 and AW24, the analyzed vortex at the lower levels is weak, due to limited V_{4RD} coverage at the low levels. As Jangmi moved near land and the inner core became well covered by the four radars in Vr4RD46 and Vr4RD06, the analyzed vortices are actually stronger and deeper than in TREC46 and TREC06. The 45 m s^{-1} contours extend to a radius of 60–70 km and reach 6 km in height (Figures 6g and 6h). In different windows, experiments assimilating V_{TREC} have compact, strong, and deep vortices with RMWs of about 30 km and a 30 m s^{-1} wind speed contour that extends as high as 8 km (Figures 6i–6l). However, the analyzed circulations are weaker than those assimilating V_{4RD} in AW46 and AW06. These results again suggest that there is benefit in directly assimilating V_r data from all available radars.

4. Combined Assimilation of V_{TREC} and V_{4RD} Data

Suggested by the results of earlier experiments, V_{TREC} and V_{4RD} are assimilated together in TRECVr and TFVR experiments, with two different configurations (Table 1). TRECVr experiments assimilate both V_{TREC} and V_{4RD} data in all cycles. Within the serial EnKF DA, V_{TREC} data are assimilated before V_{4RD} data. In TFVR (V_{TREC} first and V_r rest) experiments, V_{TREC} data are assimilated in the first cycle, while V_{4RD} data are assimilated for the remaining cycles. Hereafter, the data sets used in TRECVr and TFVR experiments are referred to as V_{TRECVr} and V_{TFVR}, respectively.

The analysis and forecast MSLPs and MSWs during the assimilation cycles for four AWs from TRECVr, TFVR, TREC, and Vr4RD experiments are plotted in Figure 7. The MSLP analyses and forecasts during DA cycles from TREC and TRECVr experiments are almost identical for all AWs, except that the MSLPs of TRECVr are slightly lower than TREC in AW24 and AW46 experiments (Figure 7a). In experiment TFVR06, higher MSLP values are obtained from 0100 through 0330 UTC, when V_{TREC} data are no longer assimilated, compared to experiments TREC06 and TRECVr06. At 0200 UTC, the analyzed MSLP in TFVR02 is about 947 hPa, which is about 10 hPa higher than in TREC02 and TRECVr02. The MSLP of TFVR06 does, however, decrease steadily and becomes slightly smaller than those of TREC06 and TRECVr06 experiments, with the final value being about 935 hPa at 0600 UTC. The MSLP values during analysis cycles of TFVR24 are also larger than those of TREC24 and TRECVr24; the final analyzed MSLP is approximately 6 hPa higher than those of TREC24 and TRECVr24. For AW46, the MSLPs from TFVR46 are similar to those of TREC46 and TRECVr46. Compared to the corresponding Vr4RD experiments, the assimilation of V_{TREC} in the first cycle generally speeds up the reduction of the analyzed MSLP significantly, especially when the V_{4RD} coverage is limited (Figure 7a).

The assimilation of V_{4RD} in addition to V_{TREC} in TRECVr experiments further improves the MSW analyses (Figure 7b) compared to TREC only experiments, which agrees with the early findings on the relative impacts of V_{4RD} and V_{TREC} assimilation on MSWs. Consistent with the MSLP results, the MSW in TFVR06 is also weaker before 0400 UTC and stronger after 0400 UTC compared to TREC06. The MSWs of TFVR24 are also weaker than TREC24 and TRECVr24, while the final MSW analysis of about 43 m s^{-1} is similar to those in TREC24 and TRECVr24. Experiment TFVR46 produces even stronger MSW analyses than TRECVr46, with the final analyzed MSW slightly overestimated compared to the ABT. In general, the assimilation of V_{TREC} at the first cycle benefits the MSW analysis, compared to experiments that assimilate Vr4RD throughout. Overall, combined assimilation of V_{TREC} and V_{4RD} data can produce better intensity analyses than assimilating them individually.

To investigate the impact of additional V_{4RD} data in the TRECVr experiments, the horizontal winds at 3 km height after the first analysis at the beginning of AW for TREC02 and TRECVr02 at 0000 UTC, TREC24 and TRECVr24 at 0200 UTC, and TREC46 and TRECVr46 at 0400 UTC are plotted in Figure 8. Due to the limited coverage of V_{4RD}, the wind analyses of TRECVr02 and TREC02 at 0000 UTC are very similar (Figures 8a and 8b). At 0200 UTC, the additional V_{4RD} data enhance the horizontal winds in the northeast quadrant of typhoon (Figures 8c and 8d). When the inner core is fully covered by V_{4RD} at 0400 UTC, the inner circulation is again noticeably enhanced by additional V_{4RD} data (Figures 8e and 8f). These results show that the additional V_{4RD}

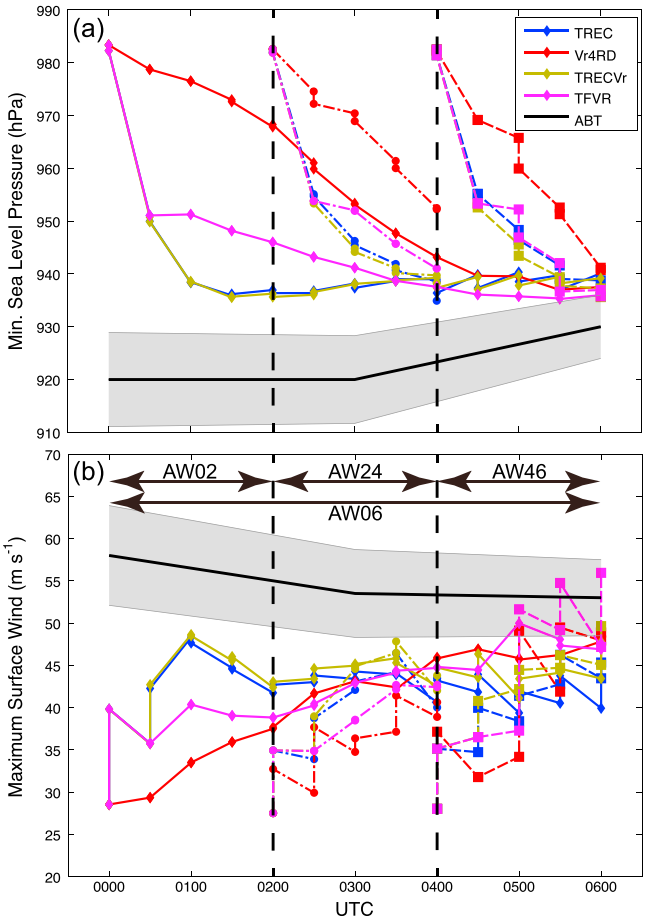

Figure 7. Analysis and forecast (a) minimum sea level pressures and (b) maximum surface winds during the analysis cycles from experiment groups TRECVr, TFVR, and TREC (in different colors) for assimilation windows of 0000 to 0600 UTC (solid lines), 0200 to 0400 UTC (dash-dotted lines), and 0400 to 0600 UTC (dashed lines). Assimilation windows (AWs) are marked by the two-way arrows. The average best track data are plotted in black for comparison. The gray shading indicates the ±1 standard deviation centered at the averaged best track.

data in TRECVr experiments do tend to further enhance the typhoon circulation, compared to the V_{TREC}-only experiments when the V_{4RD} data coverage is good.

In Figure 9, we plot the azimuthally averaged tangential wind and temperature anomaly from TRECVr and TFVR to examine the vertical structure of the final analyses. Compared to corresponding TREC experiments (Figures 6i–6l), the axisymmetric circulations of TRECVr experiments (Figures 9a–9d) are generally enhanced by the additional V_{4RD} data. The azimuthal averaged tangential wind speed of over 45 m s^{-1} is extended to a higher level, especially for AW46 and AW06. The warm core location and intensity in the TRECVr experiments are similar to those of TREC experiments but stronger than in Vr4RD experiments (Figures 6 and 9). With AW02, the axisymmetric structure of TFVR02 is much stronger than that of Vr4RD02 while weaker than TREC02 (Figure 9e), which is consistent with the MSLP analyses. For AW24, the axisymmetric circulation of TFVR24 (Figure 9f) at low levels is enhanced compared to Vr4RD24 (Figure 6f) but still weaker compared to TRECVr24 (Figure 9b). The analyzed vertical structures in TFVR46 and TFVR06 (Figures 9g and 9h) are similar to those in Vr4RD46 and Vr4RD06 (Figures 6g and 6h), suggesting that V_{4RD} data in the latter cycles play a more dominant role.

Overall, assimilating both V_{TREC} and V_r data produces better intensity and structure analyses than assimilating V_{TREC} or V_{4RD} data individually. By assimilating V_{TFVR}, the analyzed intensity and structure are also improved compared to V_{4RD} assimilation. Although the vortices from TFVR experiments are still weaker than TREC experiments for AW02 and AW24 due to relatively short windows and/or not so good V_{4RD} data coverage, the TFVR experiments for AW46 and AW06 that have much better V_{4RD} data coverage in later cycles have slightly better intensity and structure analyses than the pure TREC experiments, suggesting that underweighting the use of V_{TREC} data when direct radial velocity data from multiple radars become available is desirable.

5. Quantitative Verification of Forecasts

The impacts of assimilating V_{TREC}, V_{HL}, V_{4RD}, V_{TRECVr}, and V_{TFVR} on the intensity and structure analyses were presented in the previous sections. In this section, the impacts on the intensity and track forecasting of typhoon Jangmi are further investigated by verifying the forecasts starting from the final ensemble mean analyses against the ABT data. The 12 h accumulated precipitation and the corresponding equitable threat

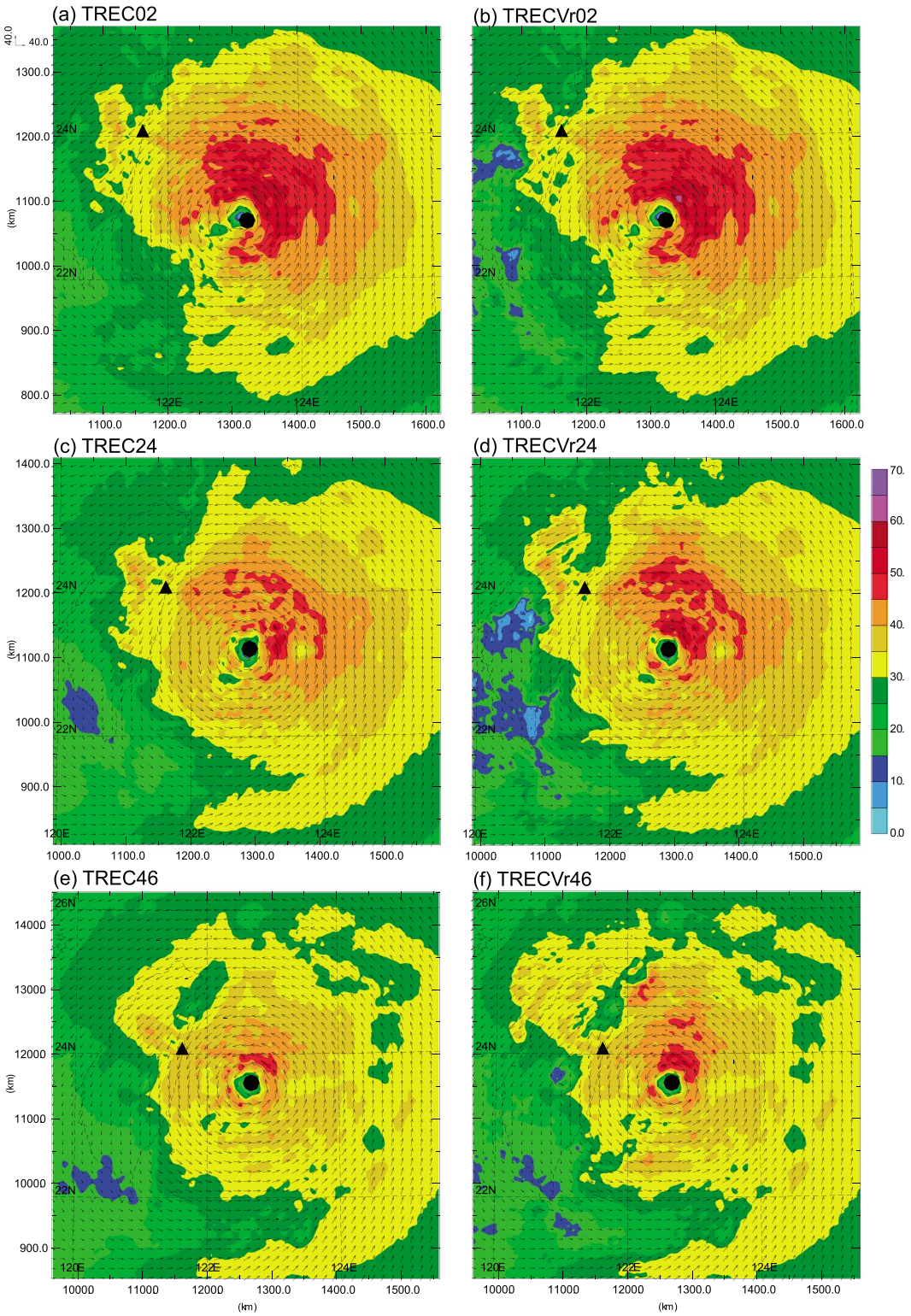

Figure 8. Horizontal wind vectors and speed (colour shaded, m s^{-1}) at 3 km height at the beginning time of the DA windows for (a) TREC02 and (b) TRECVr02 at 0000 UTC, (c) TREC24 and (d) TRECVr24 at 0200 UTC, (e) TREC46, and (f) TRECVr46 at 0400 UTC. The black dot in the panels denotes the observed typhoon center.

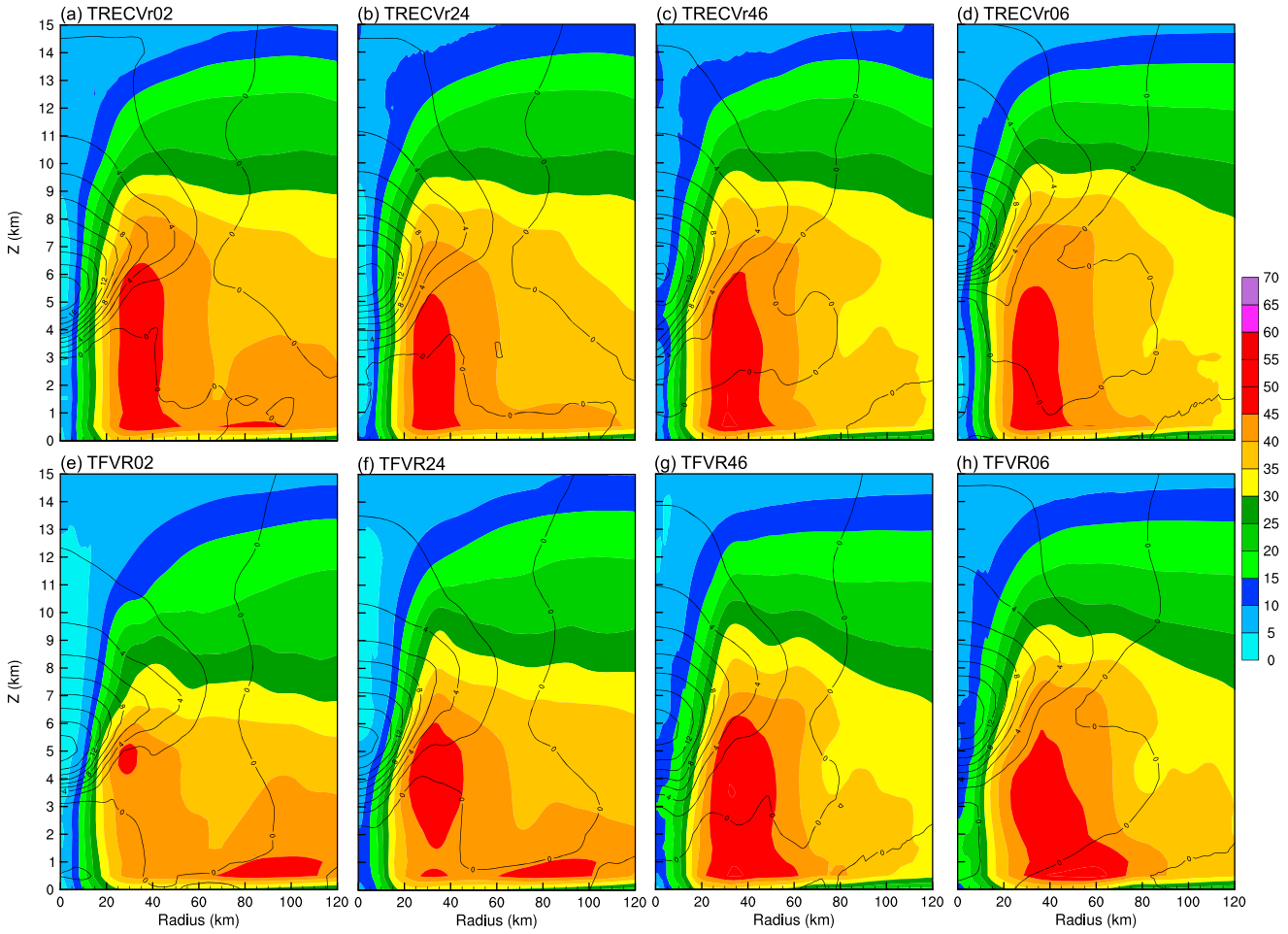

Figure 9. Azimutally averaged tangential wind (color shaded) and temperature anomaly (contours with intervals of 2 K) at the final analysis times of (a–d) the TRECVr group and (e–h) the TFVR group.

scores [ETS; *Gandin and Murphy*, 1992] from all experiments are verified against the observations. The observed rainfall is obtained from the quantitative precipitation estimation and segregation using multiple sensor system [*Gourley et al*., 2002] provided by the Central Weather Bureau of Taiwan.

5.1. Verification of Intensity and Track Forecasts Against the ABT

The predicted typhoon tracks, MSLPs, MSWs from CNTL, Vr4RD, and TREC experiments are plotted along with the ABT in Figure 10. From 0000 UTC 28 September to 0600 UTC 29 September, Jangmi first moved toward northwest, then turned into a more westward path toward Taiwan. After making landfall at about 08:30 UTC, Jangmi turned northwestward, it further turned toward north-northeast right after its center passed over Taiwan Island (Figure 10a). The track of CNTL has a large westward and southward bias with a mean track error of about 65 km. All three turns of Jangmi's track are captured well by the Vr4RD experiments at locations close to the ABT, with the mean track errors of around 50 km for the four assimilation windows. With the earlier AW02, assimilating V_{TREC} produces the track forecast that is close to that of Vr4RD. A northeastward track bias starts to show up and increase with the later AWs when assimilating V_{TREC}. The predicted track of TREC24 still captures the three turns, but the first westward turn is too weak, and the mean forecast track error is 65 km. In TREC46 and TREC06 that assimilate V_{TREC} data until 0600 UTC, the first and second turns are completely missing and the mean 24 h track errors are 70–80 km. A detailed analysis on the cause of the large track errors in TREC46 and TREC06 is the subject of a follow-on study. Initial analyses suggest that the asymmetric circulation was not retrieved accurately in the T-TREC winds, which affected the subsequent tracking forecasting.

The typhoon intensity in CNTL is too weak compared to ABT and does not change much during the forecast period. The intensity forecasts are significantly improved in Vr4RD and TREC experiments compared to CNTL.

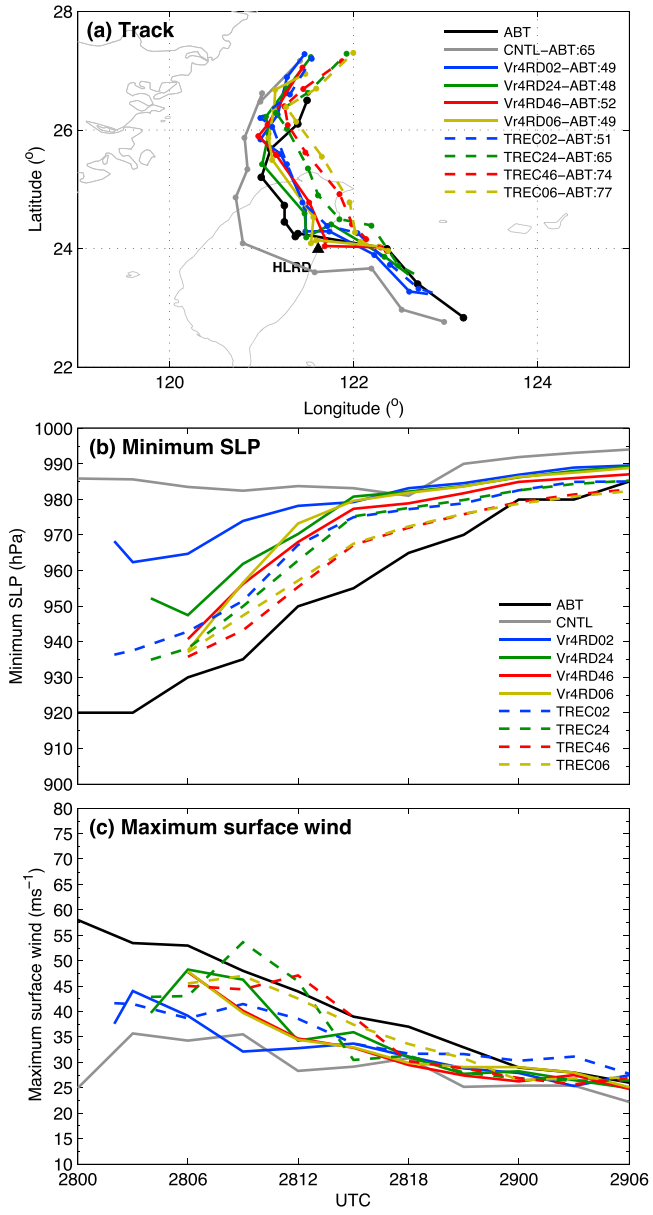

Figure 10. The predicted (a) tracks, (b) minimum sea level pressures, and (c) maximum surface winds from 0200 (Vr4RD02 and TREC02), 0400 (Vr4RD24 and TREC24), 0600 (Vr4RD46, TREC46, Vr4RD06, and TREC06) UTC 28 September to 0600 UTC 29 September 2008, and CNTL experiment, along with the average best track (ABT, see section 2). The dots in Figure 10a denote the center locations every 3 h starting from 0000 UTC 28 September. The ABT at 0200 and 0400 UTC 28 is linear interpolated from available time. The numbers in Figure 10a denote the mean track errors over the forecast period against the ABT.

The forecasts of TREC experiments are, in general, closer to the ABT than those of Vr4RD experiments in terms of both MSLP and MSW (Figures 10b and 10c). The TREC46 and TREC06 experiments have the best (strongest) intensity forecasts among all experiments, but their stronger vortices are at least partly due to the northward bias of the forecast track, which almost missed landfall.

To further quantify the forecast quality, the 24 h average MSLP, MSW, and track errors from the VrHL, Vr4RD, TREC, TRECVr, and TFVR DA experiments for all AWs are plotted in Figure 11 along with those of CNTL experiment that did not perform radar DA. The group mean errors for every group of experiments (e.g., the mean of the 24 hour averaged MSLP errors from Vr4RD experiments, including Vr4RD02, Vr4RD24, Vr4RD46, and Vr4RD06) are also plotted to provide a synopsis on track and intensity errors. The group mean here is just an indicator for the average performance of each data type for various assimilation windows; it does not necessarily have much physical meaning given that it is the average of experiments with different assimilation window lengths. It is clear that V_{4RD} assimilation produces better intensity and track forecast than V_{HL} assimilation for every AW. The V_{4RD}-assimilating group mean MSLP, MSW, and track errors are 17.2 hPa, 5.5 m s^{-1}, and 49 km, respectively, compared to the 20 hPa, 8.3 m s^{-1}, and 61 km of the VrHL group (Figure 11).

The northeast track bias of TREC experiments is largely corrected by assimilating V_{4RD} data in addition: the westward track deflection at 0600 UTC is better captured by TRECVr46 and TRECVr06 (not shown) than the corresponding TREC experiments, resulting in smaller track errors (Figure 11c). The TRECVr group mean track error is reduced to about 59 km. Meanwhile, TFVR experiments well predict all three turns of Jangmi's track (not shown). The track forecasts of TFVR experiments are comparable to those of Vr4RD experiments, with a group mean error of about 49 km (Figure 11c). Compared to the TREC and TRECVr experiments, the TFVR experiments generally have much better track forecasts.

Assimilating V_{TREC} and V_{4RD} together in TRECVr experiments gives better track forecasts than TREC experiments and much improved intensity forecasts over Vr4RD experiments. The group mean intensity error is

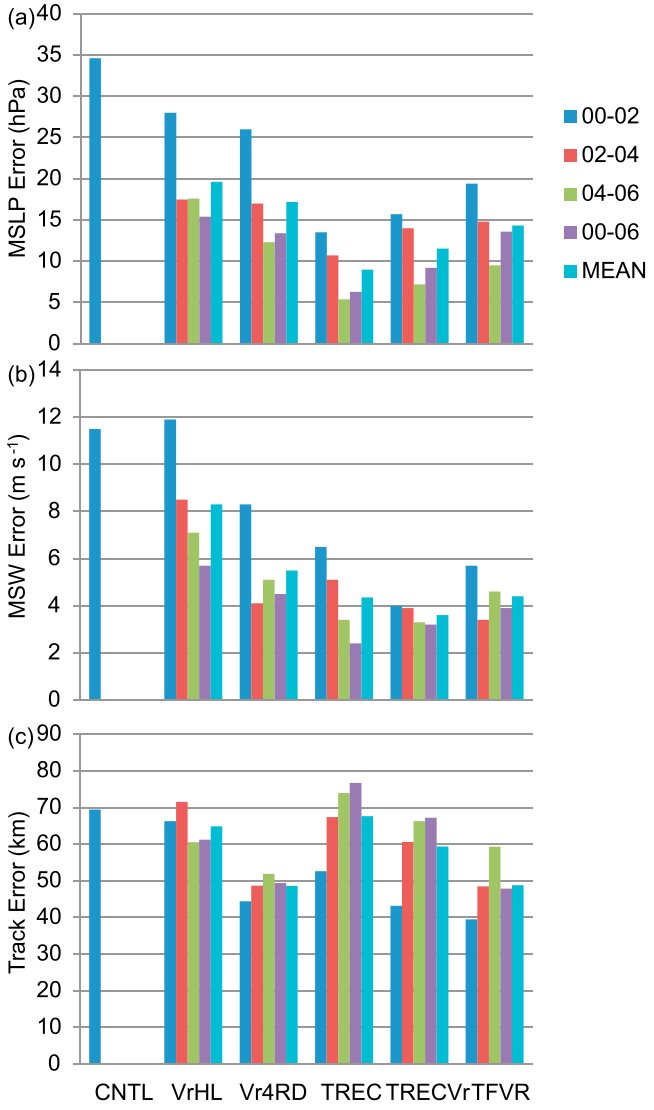

Figure 11. The 24 h averaged forecast (a) MSLP errors, (b) MSW errors, (c) and track errors from different groups of experiments.

more than 30% smaller than that of Vr4RD group (Figures 11a and 11b). The assimilation of V_{TREC} in the first cycle in TFVR experiments improves the intensity forecasts compared to Vr4RD experiments (Figures 11a and 11b). The group mean MSLP and MSW errors are approximately 14 hPa and 4.4 m s^{-1}, respectively, that are about 20% smaller than those of Vr4RD.

In this particular case of typhoon Jangmi, the intensity and precipitation forecasts depend largely on the track forecast. The track forecast, especially the westward turn at 0600 UTC, can be more important than the general intensity forecast. A "good" intensity forecast with a highly biased track forecast should not be considered as a good TC forecast since wrong areas will be affected. Among all DA experiments, TFVR and Vr4RD have the best track forecasts with the group errors being about 49 km in both cases. The track forecasts from TREC experiments are too biased. TFVR has smaller group mean MSLP and MSW errors of 14 hPa and 4.4 m s^{-1}, smaller than the 17.2 hPa and 5.5 m s^{-1} of the Vr4RD group. The improvement to intensity forecast from TFVR over Vr4RD is even larger with the earlier AW02 and AW24 (Figures 11a and 11b). These results suggest that the configuration that assimilates V_{TREC} in the first cycle and V_r in later cycles has the potential to improve both track and intensity forecasts of TCs.

5.2. Verification of Precipitation

The 12 h accumulated precipitations from all experiments are presented in Figure 12 together with the observations. Figures 12a–12x represent precipitation forecasts from earlier to later AWs. For the 12 h accumulated precipitation valid at 1400 UTC (Figures 12a–12f), prominent in the data is a strong precipitation band along the central mountain region (Figures 1 and 12a); two precipitation maxima are located over northern and southern Taiwan (separated by the 24°N). These observed maxima are significantly underpredicted in VrHL02 and Vr4RD02 (Figures 12b and 12c) but better predicted by TREC02, TRECVr02, and TFVR02 (Figures 12d–12f). The northern rainfall maximum is best captured by TREC02, while the TRECVr02 has the best forecast of the southern rainfall maximum. After 2 h, the 12 h accumulated rainfall ending at 1600 UTC shifted somewhat to the south (Figure 12g). There is still underprediction of the two precipitation centers in all forecasts. TRECVr24 and TFVR24 predict the north and south centers, respectively, better than others. Ending at 1800 UTC (Figures 12g–12l and 12m–12r), observed 12 h precipitation continues to shift to the south, resulting in very heavy precipitation around 23.5°N, Taiwan. This heavy precipitation pattern is well captured by VrHL46, Vr4RD46, VrHL06, and Vr4RD06, but the rainfall amount is too low (Figures 12n, 12o, 12t, and 12u). The predicted rainfall location, pattern, and magnitude in TFVR06 over southern Taiwan

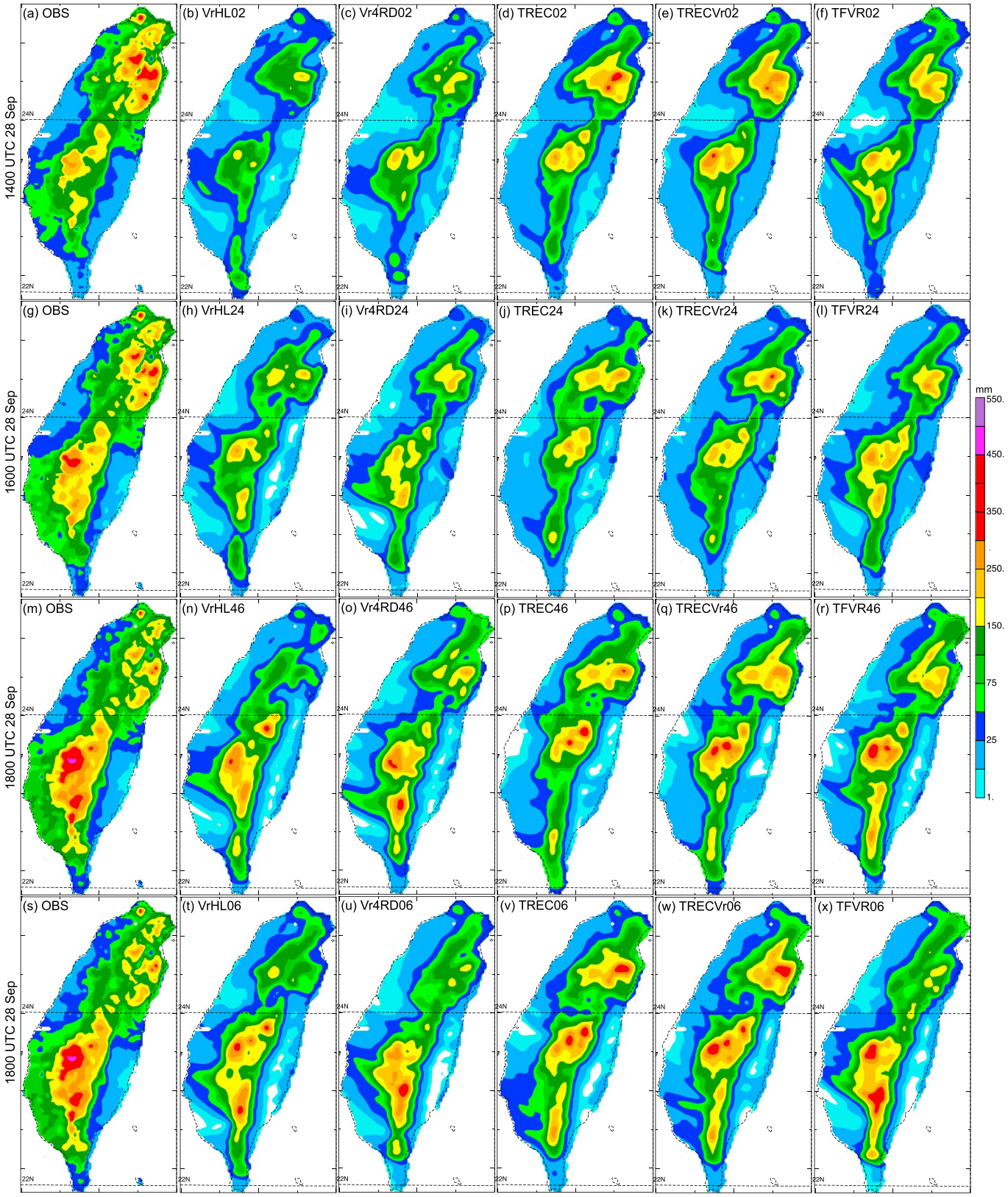

Figure 12. A 12 h accumulated precipitation for (a, g, m, and s) observations, (b, h, n, and t) VrHL group, (c, i, o, and u) Vr4RD group, (d, j, p, and v) TREC group, (e, k, q, and w) TRECVr group, and (f, l, r, and x) TFVR group. Figures 12a–12f, 12g–12l, 12m–12r, and 12s–12x are valid at 1400 UTC, 1600 UTC, 1800 UTC, and 1800 UTC 28 September, respectively.

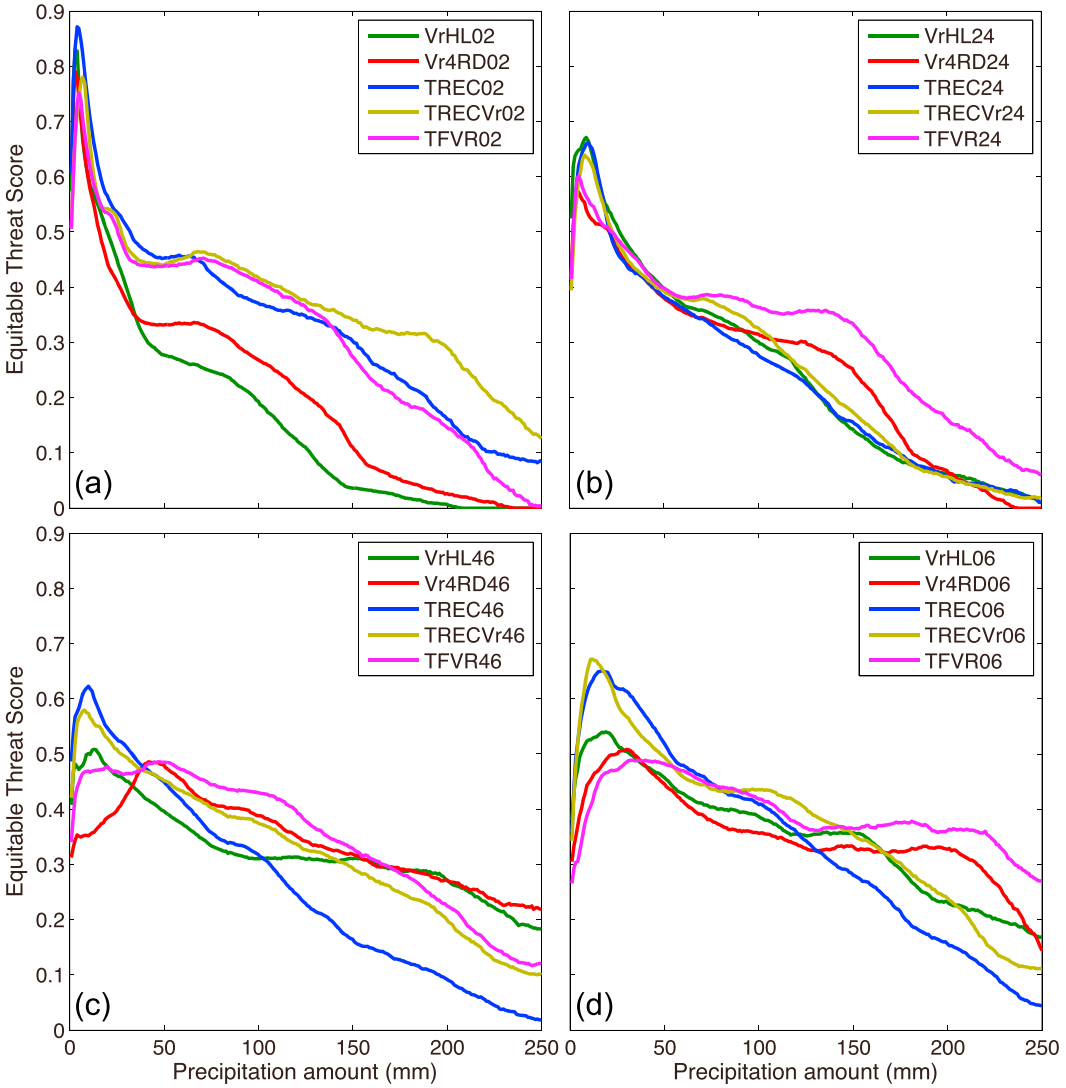

Figure 13. Equitable threat scores of the 12 h accumulated precipitation forecasts from experiments of different assimilation windows, (a) 0000–0200 UTC, (b) 0200–0400 UTC, (c) 0400–0600 UTC, and (d) 0000–0600 UTC.

appear to be closest to the observations among the accumulations ending at 1800 UTC. As a result of their northward biased tracks, TREC46, TRECVr46, and TFVR46 predict precipitation in northern Taiwan that happens to match observations quite well, but the precipitation over southern Taiwan has large northward biases (Figures 12p–12r). The same is true with TREC06 and TRECVr06, and over northern Taiwan the predicted precipitation is too strong (Figures 12v and 12w).

The ETSs of the 12 h accumulated precipitation for experiments with different AWs are plotted in Figure 13. For AW02, VrHL02, and Vr4RD02 have low ETSs for all rainfall thresholds, corresponding to previously noted underprediction of precipitation (Figure 13a). The ETSs of TRECVr02 are generally the highest among this group of experiments, especially for heavier precipitation (>150 mm). For AW24, the spread of ETSs is greatly reduced, partly due to improvements in VrHL24 and Vr4RD24, which benefited from improved V_r data coverage. TFVR24 now has the highest ETSs for most thresholds in this group of experiments (Figure 13b). For AW46, the ETSs of TREC46 are the lowest, in general, due to the large track error. Other experiments have comparable ETSs (Figure 13c). For the long 6 h window AW06, the ETSs of TREC06 are the lowest for strong precipitation while those of TFVR06 are the highest for strong precipitation (Figure 13d). For weaker precipitation, the differences are smaller.

To highlight the general relative impacts of assimilating different data groups, the group mean ETSs of the 12 h accumulated precipitation from VrHL, Vr4RD, TREC, TRECVr, and TFVR are presented in Figure 14. Generally, the

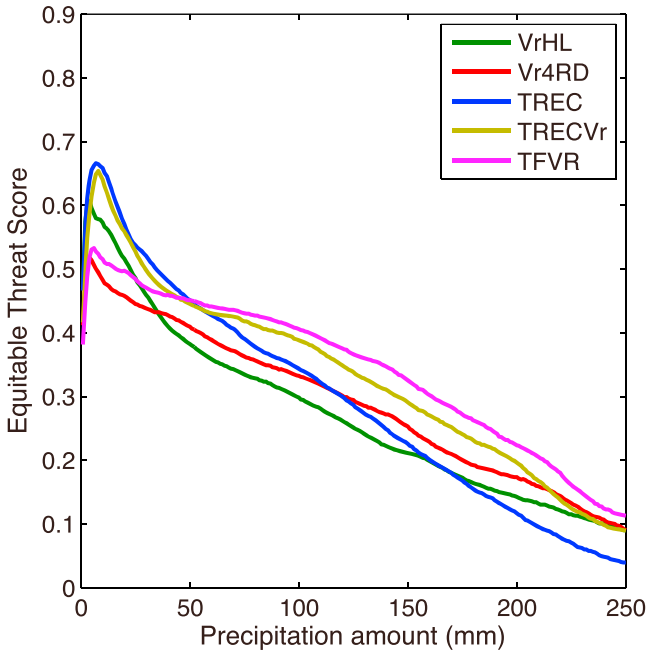

Figure 14. The averaged equitable threat scores of the 12 h accumulated precipitation forecasts from assimilation groups VrHL, Vr4RD, TREC, TRECVr, and TFVR.

TFVR group has the highest ETSs for thresholds above 50 mm; this group hence has the best precipitation forecast skill. This can be attributed to the best intensity and track forecasts the group has. The assimilation of both V_{TREC} and V_{4RD} in TRECVr also gives higher ETSs than assimilating V_{TREC} or V_{4RD} only. Consistent with the intensity and track forecasting results, the precipitation forecasts of Vr4RD group are also better than those of VrHL group.

6. Summary and Discussion

W14 compared the assimilation of V_{TREC} versus V_r data from a single Doppler radar on the Taiwan Island over a 1, 2, or 3 h window after the center of Typhoon Jangmi (2008) first moved into the radial velocity coverage of the radar. Thirty-minute assimilation cycles were used with an ensemble Kalman filter. Results demonstrated that V_{TREC} assimilation is more effective than V_r assimilation and thus can potentially provide better TC initialization and improved forecasts with longer lead times than V_r data can. The larger spatial coverage of V_{TREC} data and the more complete wind information (including cross-beam component) it contains are believed to be the primary reasons for the superior performance of V_{TREC} over V_r data.

As a follow-up to W14, this study further examines the relative impacts of assimilating V_r, V_{TREC} or their combinations in assimilation windows (AWs) that span different time periods before Jangmi landfall over Taiwan. Specifically, data during 0000 UTC to 0600 UTC 28 September 2008 from four coastal operational Doppler radars located at Hualian (HLRD), Wufenshan (WFRD), Chigu (CGRD), and Kenting (KTRD) of Taiwan are used. The 6 h window is further split into three 2 h windows, in which V_r data from the radars have different degrees of coverage on the TC inner core region. Four sets of experiment are performed that have, respectively, AWs of 0000 to 0200 UTC (AW02), 0200 to 0400 UTC (AW24), 0400 to 0600 UTC (AW46), and 0000 to 0600 UTC (AW06). Assimilation cycles are again 30 min long in all cases. For each set of experiments, five forms of data are assimilated; they are V_r from HLRD radar only (labeled V_{HL}), V_r from all four radars (labeled V_{4RD}), T-TREC-retrieved winds (V_{TREC}), both V_{TREC} and V_{4RD} (labeled V_{TRECVr}) in every cycle, and V_{TREC} in the first cycle and V_{4RD} in the remaining cycles (labeled V_{TFVR}).

The assimilation of V_{TREC} data (derived from the reflectivity data of Hualian radar) generally produces better intensity and structure analyses of the typhoon than V_{HL} for all AWs due to the added cross-beam wind information and the larger data coverage. Even for the 6 h AW that has better V_{HL} coverage near the end, the advantage of assimilating V_{TREC} is still evident. The assimilation of V_{4RD} also produces better intensity and structure analyses than V_{HL} for all AWs. For earlier AWs when the inner core is only partly covered by V_{4RD}, V_{TREC} assimilation produces better intensity and structure analyses than V_{4RD} assimilation. When the inner core region has very good V_{4RD} coverage (in AW46 and AW06), Vr4RD experiments improve the structure and maximum surface wind analyses compared to corresponding TREC experiments.

For V_r assimilation, the more V_r observations in the inner core region are assimilated, the better are the intensity and structure analyses obtained. The assimilation of V_{4RD} and V_{HL} within the 6 h AW produces better analyses than 2 h AWs; a later 2 h AW window with a better V_r coverage also leads to a better analysis. However, the assimilation of V_{TREC} is not sensitive to the AW used because it can spin up strong typhoon vortex quickly within 1 h.

The trade-off between V_{TREC} and V_{4RD} assimilation indicated the potential benefit of assimilating V_{TREC} and V_{4RD} together. Doing so is found to improve the analyzed typhoon intensity and the axisymmetric circulation

compared to assimilating V_{TREC} or V_{4RD} alone. Assimilating V_{TREC} in the first cycle then V_{4RD} in the remaining cycles (V_{TFVR} assimilation) improves the typhoon intensity and structure analyses compared to always assimilating V_{4RD}, especially for AW02 and AW24. However, assimilating V_{TREC} still produces better intensity and structure analyses than V_{TFVR} assimilation for AW02 and AW24.

In the case of typhoon Jangmi, track forecast is important as it affects the landfall time and location and hence also intensity and precipitation forecasts. Consistent with the quality of intensity and structure analyses, the V_{4RD} assimilation also leads to better forecasts than V_{HL} assimilation in terms of both track and intensity. The assimilation of V_{TREC} produces overall the best intensity forecasts among all DA experiments as it is quick at establishing a strong vortex, but the track forecast errors of V_{TREC} DA experiments are the largest overall. This large track error is believed to be due to the inaccurately retrieved asymmetric circulation associated with the increasing T-TREC retrieval error the Jangmi precipitation is partially over land [*Wang et al*., 2014]. The assimilation of V_{4RD} in addition to V_{TREC} substantially improves the track forecasts compared to V_{TREC} assimilation only; however, the track error is still much larger than V_{4RD} DA experiments. V_{TFVR} and V_{4RD} DA experiments produce the best track forecasts, while V_{TFVR} experiments have better intensity forecasts due to the improved intensity analysis compared to V_{4RD} experiments. In general, the V_{TFVR} assimilation leads to the best track and intensity forecasts among all DA experiments.

Qualitative and quantitative evaluations of precipitation forecasts also show that V_{TFVR} experiments have the highest precipitation forecast skills for moderate to heavy precipitation, which is consistent with the best track and intensity forecasts. The assimilation of V_{TREC} and V_{4RD} together also gives higher precipitation forecast skills than assimilating V_{TREC} or V_{4RD} alone. Although the intensity and track forecasting behaviors are different, V_{TREC} and V_{HL} DA experiments generally have similar, lower precipitation forecast skills. Considering the intensity, track, and precipitation forecasts together, the assimilation of V_{TREC} data in the first cycle and then assimilating V_r data from all four available radars in the remaining cycles produce most positive impact on Jangmi forecasting near Taiwan.

Based on the results of experiments performed in this study, some recommendations for radar data assimilation configuration for a typhoon approaching coastal radars are made here: When a good reflectivity data coverage is available from a coastal radar on a approaching typhoon, T-TREC wind retrievals are to be performed. The retrieved T-TREC winds are assimilated in the first one or two cycles using an advanced data assimilation method such as the EnKF; the assimilation can usually establish the typhoon vortex circulation quite well. As the typhoon moves closer to the coast, V_r data coverage from the coastal radars improves; the assimilation of V_r data is then preferred over the often less accurate T-TREC data, especially when multi-Doppler radar coverage is available. The original V_r data usually contain more circulation details than T-TREC retrievals. However, because this recommendation is based on the results of a single case, and a specific radar network, the generality of the results will require testing with more cases, in future studies. To understand why the track forecasts starting from the analyses of T-TREC assimilation experiments were poorer in this case, detailed analyses will be performed and reported in a follow-on paper.

Acknowledgments

This work was primarily supported by the National 973 Fundamental Research Program of China (2013CB430103), DOD-ONR grant N00014-10-1-0775, Social Common Wealth Research Program (GYHY201006007), and the National Natural Science Foundation of China (grants 41275031 and 41322032). The second author acknowledges the support of NSF grants AGS-0802888, AGS-1046171, and AGS-1261776. The data sets used in this study are available on a cloud drive. The url is http://pan.baidu.com/s/1bnCyV8b with password 7152.

References

Barker, D. M., W. Huang, Y. R. Guo, A. J. Bourgeois, and Q. N. Xiao (2004), A Three-dimensional variational data assimilation system for MM5: Implementation and initial results, *Mon. Weather Rev.*, *132*(4), 897–914.

Blackwell, K. G. (2000), The evolution of Hurricane Danny (1997) at landfall: Doppler-observed eyewall replacement, vortex contraction/intensification, and low-level wind maxima, *Mon. Weather Rev.*, *128*(12), 4002–4016.

Corbosiero, K. L., J. Molinari, A. R. Aiyyer, and M. L. Black (2006), The structure and evolution of Hurricane Elena (1985). Part II: Convective asymmetries and evidence for vortex Rossby waves, *Mon. Weather Rev.*, *134*(11), 3073–3091.

Deardorff, J. (1980), Stratocumulus-capped mixed layers derived from a three-dimensional model, *Boundary Layer Meteorol.*, *18*(4), 495–527.

Dong, J., and M. Xue (2013), Assimilation of radial velocity and reflectivity data from coastal WSR-88D radars using an ensemble Kalman filter for the analysis and forecast of landfalling hurricane Ike (2008), *Q. J. R. Meteorol. Soc.*, *139*(671), 467–487.

Gandin, L. S., and A. H. Murphy (1992), Equitable skill scores for categorical forecasts, *Mon. Weather Rev.*, *120*(2), 361–370.

Gourley, J. J., R. A. Maddox, K. W. Howard, and D. W. Burgess (2002), An exploratory multisensor technique for quantitative estimation of stratiform rainfall, *J. Hydrometeorol.*, *3*(2), 166–180.

Hong, J.-S., and P.-L. Chang (2005), The trochoid-like track in Typhoon Dujuan (2003), *Geophys. Res. Lett* , *32* L16801, doi:10.1029/2005GL023387.

Lee, W. C., and M. M. Bell (2007), Rapid intensification, eyewall contraction, and breakdown of Hurricane Charley (2004) near landfall, *Geophys. Res. Lett.*, *34* L02802, doi:10.1029/2006GL027889.

Lee, W.-C., B. J. D. Jou, P.-L. Chang, and F. D. Marks (2000), Tropical cyclone kinematic structure retrieved from single-doppler radar observations. Part III: Evolution and structures of Typhoon Alex (1987), *Mon. Weather Rev.*, *128*(12), 3982–4001.

Li, X., J. Ming, Y. Wang, K. Zhao, and M. Xue (2013), Assimilation of T-TREC-retrieved wind data with WRF 3DVAR for the short-term forecasting of typhoon Meranti (2010) near landfall, *J. Geophys. Res. Atmos.*, *118*, 10,361–310,375, doi:10.1002/jgrd.50815.

Li, Y., X. Wang, and M. Xue (2012), Assimilation of radar radial velocity data with the WRF hybrid ensemble—3DVAR system for the prediction of Hurricane Ike (2008), *Mon. Weather Rev.*, *140*(11), 3507–3524.

Lin, Y.-L., R. D. Farley, and H. D. Orville (1983), Bulk parameterization of the snow field in a cloud model, *J. Climate Appl. Meteorol.*, *22*(6), 1065–1092.

Liu, Y., D.-L. Zhang, and M. K. Yau (1999), A multiscale numerical study of hurricane Andrew (1992). Part II: Kinematics and inner-core structures, *Mon. Weather Rev.*, *127*(11), 2597–2616.

Ren, D., and M. Xue (2004), A Revised force–restore model for land surface modeling, *J. Appl. Meteorol.*, *43*(11), 1768–1782.

Tuttle, J., and R. Gall (1999), A single-radar technique for estimating the winds in tropical cyclones, *Bull. Am. Meteorol. Soc.*, *80*(4), 653–668.

Wang, M., K. Zhao, and D. Wu (2011), The T-TREC technique for retrieving the winds of landfalling typhoons in China, *Acta Meteorol. Sin.*, *25*(1), 91–103.

Wang, M., M. Xue, K. Zhao, and J. Dong (2014), Assimilation of T-TREC-Retrieved winds from single-doppler radar with an ensemble Kalman filter for the forecast of Typhoon Jangmi (2008), *Mon. Weather Rev.*, *142*(5), 1892–1907.

Whitaker, J. S., and T. M. Hamill (2012), Evaluating methods to account for system errors in ensemble data assimilation, *Mon. Weather Rev.*, *140*(9), 3078–3089.

Xiao, Q., K. Ying-Hwa, J. Sun, W.-C. Lee, E. Lim, Y.-R. Guo, and D. M. Barker (2005), Assimilation of Doppler radar observations with a regional 3DVAR system: Impact of Doppler velocities on forecasts of a heavy rainfall case, *J. App. Meteorol.*, *44*, 768–788.

Xiao, Q., Y.-H. Kuo, J. Sun, W.-C. Lee, D. M. Barker, and E. Lim (2007), An approach of radar reflectivity data assimilation and its assessment with the inland QPF of Typhoon Rusa (2002) at landfall, *J. Appl. Meteorol. Climatol.*, *46*(1), 14–22.

Xue, M., and J. Dong (2013), Impact of assimilating best track minimum sea level pressure data together with coastal Doppler radar data on hurricane analysis and prediction at a cloud-resolving resolution, *Acta Meteorol. Sin.*, *27*(3), 379–399.

Xue, M., J. Zong, and K. K. Droegemeier (1996), Parameterization of PBL turbulence in a multi-scale non-hydrostatic model paper presented at Preprint, 11th AMS Conf. Num. Wea. Pred., *Am. Meterol. Soc.*, Norfolk, Va.

Xue, M., K. K. Droegemeier, and V. Wong (2000), The Advanced Regional Prediction System (ARPS)—A multi-scale nonhydrostatic atmospheric simulation and prediction model. Part I: Model dynamics and verification, *Meteorol. Atmos. Phys.*, *75*(3–4), 161–193.

Xue, M., K. K. Droegemeier, V. Wong, A. Shapiro, K. Brewster, F. Carr, D. Weber, Y. Liu, and D. Wang (2001), The Advanced Regional Prediction System (ARPS)—A multi-scale nonhydrostatic atmospheric simulation and prediction tool. Part II: Model physics and applications, *Meteorol. Atmos. Phys.*, *76*(3–4), 143–165.

Zhang, F., Y. Weng, J. A. Sippel, Z. Meng, and C. H. Bishop (2009), Cloud-resolving hurricane initialization and prediction through assimilation of doppler radar observations with an ensemble Kalman filter, *Mon. Weather Rev.*, *137*(7), 2105–2125.

Zhao, K., and M. Xue (2009), Assimilation of coastal Doppler radar data with the ARPS 3DVAR and cloud analysis for the prediction of Hurricane Ike (2008), *Geophys. Res. Lett.*, L12803, doi:10.1029/2009GL038658.

Zhao, K., W. C. Lee, and B. J. D. Jou (2008), Single Doppler radar observation of the concentric eyewall in Typhoon Saomai, 2006, near landfall, *Geophys. Res. Lett.*, *35*, L07807, doi:10.1029/2007GL032773.

Zhao, K., X. F. Li, M. Xue, B. J. D. Jou, and W. C. Lee (2012), Short-term forecasting through intermittent assimilation of data from Taiwan and mainland China coastal radars for Typhoon Meranti (2010) at landfall, *J. Geophys. Res.*, *117* D06108, doi:10.1029/2011JD017109.

Zhao, Q., and Y. Jin (2008), High-resolution radar data assimilation for Hurricane Isabel (2003) at landfall, *Bull. Am. Meteorol. Soc.*, *89*, 1355–1372.